Atmospheric Environment 225 (2020) 117370

Contents lists available at ScienceDirect

Atmospheric Environment

journal homepage: http://www.elsevier.com/locate/atmosenv

Comparison of solid phase extraction methods for the measurement of humic-like substances (HULIS) in atmospheric particles

Chunlin Zou [a,b], Meiju Li [a,b], Tao Cao [a,b], Mengbo Zhu [a,b], Xingjun Fan [c], Shiyun Peng [a,b], Jianzhong Song [a,*], Bin Jiang [a], Wanglu Jia [a], Chiling Yu [a], Haiyan Song [d], Zhiqiang Yu [a], Jun Li [a], Gan Zhang [a], Ping'an Peng [a,b]

[a] State Key Laboratory of Organic Geochemistry and Guangdong Key Laboratory of Environmental Protection and Resources Utilization, Guangzhou Institute of Geochemistry, Chinese Academy of Sciences, Guangzhou, 510640, China
[b] University of Chinese Academy of Sciences, Beijing, 100049, China
[c] College of Resource and Environment, Anhui Science and Technology University, Fengyang, 233100, China
[d] School of Chemistry and Environment, South China Normal University, Universities Town, Guangzhou, 510006, PR China

HIGHLIGHTS

- HLB-M, HLB-N, and PPL methods are comparatively investigated and estimated.
- All SPE methods were favorable for high UV absorbance and aromatic compounds.
- Some HULIS molecules were changed during the HLB-N treatment.
- The PPL method serves equally good for HULIS isolation and characterization.

ARTICLE INFO

Keywords:
HULIS
Isolation
PPL
HLB-M
HLB-N

ABSTRACT

Humic-like substances (HULIS) constitute a significant fraction of the water-soluble organic compounds in the environment and influence many properties of atmospheric aerosols. In this study, three solid phase extraction (SPE) methods that involve the use of hydrophilic/lipophilic balanced (HLB) resin with pure methanol (HLB-M), HLB resin with 2% (v/v) ammonia/methanol (HLB-N), and Bond Elut PPL (Priority PolLutant) resin with methanol (PPL), were compared for the isolation of HULIS from atmospheric aerosols. The HLB-N and PPL methods efficiently recovered Suwannee River fulvic acid (SRFA) and were excellent for quantifying HULIS at low levels in aerosols. All three SPE methods were favorable for the elution of aromatic and strongly UV-absorbing compounds. However, the chemical structures and molecular compositions of the HULIS isolated by the three methods showed some differences. The $HULIS_{HLB\text{-}N}$ and $HULIS_{PPL}$ fractions contained higher concentrations of aliphatic and aromatic C–H groups than did the $HULIS_{HLB\text{-}M}$ fraction, indicating that relative higher content of weak polar organic species in HULIS fractions isolated by the HLB-N and PPL methods than those isolated by the HLB-M method. Moreover, the $HULIS_{HLB\text{-}N}$ and $HULIS_{PPL}$ were both characterized by having lower relative abundance-weighted modified aromaticity index values and higher concentrations of S-containing compounds than the $HULIS_{HLB\text{-}M}$, as indicated by Fourier transform ion cyclotron resonance mass spectrometry. Some N-containing structures were identified only in the $HULIS_{HLB\text{-}N}$, suggesting that some of HULIS molecules were changed during the HLB-N treatment. Based on these comparisons of the three methods, we found that the PPL method serves equally good as compared to other two methods, and therefore, one can utilize PPL method also for HULIS isolation and characterization.

1. Introduction

Humic-like substances (HULIS), a class of water-soluble organic compounds in atmospheric samples, have certain features (e.g., UV–Vis absorbance, fluorescence, and nuclear magnetic resonance (NMR) characteristics) similar to those of natural humic and fulvic acids

* Corresponding author.
E-mail address: songjzh@gig.ac.cn (J. Song).

https://doi.org/10.1016/j.atmosenv.2020.117370
Received 8 October 2019; Received in revised form 18 February 2020; Accepted 23 February 2020
Available online 26 February 2020

(Graber and Rudich, 2006; Win et al., 2018). These substances are ubiquitous in the atmospheric aerosols, cloudwater, fogwater, and rainwater in various environments and account for a significant portion of the water-soluble organic compounds (Duarte et al., 2007; Lin et al., 2010; Song et al., 2012; Zheng et al., 2013). Because of their strong light-absorbing properties, water solubility, and surface activity, HULIS have a strong effect on the formation of cloud condensation nuclei and aerosol hygroscopicity and affect the scattering and light absorption of aerosols; therefore, they have a substantial impact on the regional atmospheric environment and climate changes (Dinar et al., 2006; Wang and Knopf, 2011). In addition, some HULIS may induce the generation of reactive oxygen species and thus have direct or indirect harmful effects on human health (Verma et al., 2012, 2015; Win et al., 2018).

It is well known that HULIS are complex organic molecules, and many methods have been used for their isolation from ambient samples (Decesari et al., 2000; Samburova et al., 2005). Among these methods, solid phase extraction (SPE) is the one most frequently used for the simultaneous concentration and isolation of HULIS from other water soluble constituents (Baduel et al., 2009; Fan et al., 2012, 2013; Lin et al., 2010; Varga et al., 2001; Zhao et al., 2016). The commonly used sorbents include HLB (hydrophilic/lipophilic balanced polymer) (Lin et al., 2010; Park and Yu, 2016; Varga et al., 2001), C-18 (Baduel et al., 2009; Verma et al., 2015), XAD-8 (Sullivan and Weber, 2006) and DEAE (diethylaminoethyl cellulose) (Baduel et al., 2009; Fan et al., 2012; Varga et al., 2001). Each sorbent has advantages and disadvantages (Fan et al., 2012, 2013; Varga et al., 2001). For example, Varga et al. (2001) proposed a comparison between the HLB and C-18 methods and reported that HLB may be the preferred method for the isolation of HULIS. In our previous studies (Fan et al., 2012, 2013), comprehensive comparisons among the ENVI-18, HLB, XAD-8, and DEAE methods were conducted, and the HLB method was found to have several advantages for the separation of HULIS in aerosols when methanol was used as the eluent (HLB resin with pure methanol, HLB-M). One of the advantages was that the properties of the HULIS were not changed during the treatment processes. However, a substantial amount of adsorbed carbon ($19 \pm 12\%$) was retained on the HLB column when methanol was used as the eluent, and this amount decreased to $4 \pm 5\%$ when 2% ammonia/-methanol was used for the elution (HLB-N) (Lin et al., 2010). The HULIS isolated using the HLB-N method also exhibited some differences from those isolated by HLB-M (Fan et al., 2013). The $HULIS_{HLB\text{-}N}$ had a relatively high N/C ratio and contained some N-containing functional groups, but these results were obtained based only on the proton nuclear magnetic resonance (^{1}H-NMR) properties, and further investigation at the molecular level is necessary.

More recently, the functionalized styrene-divinylbenzene polymer (Bond Elut Priority PolLutant resin, PPL) sorbent has been widely utilized to isolate dissolved organic matter from ocean water samples (Dittmar et al., 2008; Green et al., 2014). The PPL resin can extract hydrophobic and less polar compounds, such as phenols, and has been shown to give a high recovery of dissolved organic matter (DOM) from river and ocean water (Dittmar et al., 2008; Li et al., 2017; Stubbins et al., 2012). Because atmospheric HULIS are a type of water-soluble organic matter and are similar to natural humic substances, the PPL method is likely to be a good choice for the isolation of water soluble HULIS from atmospheric samples.

The aim of this study was to develop a reliable method for the isolation and characterization of HULIS in atmospheric aerosols, based on previous studies of the isolation of atmospheric HULIS (Baduel et al., 2009; Sullivan and Weber, 2006; Varga et al., 2001). Thus, the fulvic acid (FA) yields from a Suwannee river fulvic acid (SRFA) solution and HULIS in aerosol water-soluble organic carbon (WSOC) isolated by the HLB method with elution by methanol (HLB-M) and 2% (v/v) ammonia/methanol (HLB-N) and the PPL method with elution by methanol (PPL) were determined by total organic carbon (TOC) and UV254 detection. Then, the chemical and molecular properties of the HULIS isolated by these three methods were examined using UV–Vis and ^{1}H-NMR spectroscopy and Fourier transform ion cyclotron resonance mass spectrometry (FT-ICR MS). The results will advance our understanding of the characteristics of each method and enable the establishment of a method that has a high extraction recovery of HULIS and causes little change in its chemical composition and structure.

2. Experimental

2.1. Materials

In this study, Suwannee river fulvic acid (SRFA) (1R101F) was used as a model for atmospheric HULIS. The sample was obtained from the International Humic Substances Society (IHSS) and was selected because of its widespread use in many studies as a representative substance for atmospheric HULIS (Baduel et al., 2009; Chalbot et al., 2014; Lin et al., 2010; Park and Yu, 2016).

Ambient aerosol samples were also used to test the three SPE methods. The aerosol samples were collected on 20.3×25.4 sq. cm Whatman quartz fiber filters with a high-volume sampler at a flow rate of 300 L/min (Mingye PM-PUF-300, Mingye Instruments, Guangzhou, China). The sampler was located approximately 30 m above ground level on the rooftop of a nine-story building at the Guangzhou Institute of Geochemistry, Chinese Academy of Sciences. The sampling was conducted January 3–5, 2016 (No. WuShan-1, abbreviated as WS1) and October 24–30, 2017 (Nos. WS2−WS7). Each sample acquisition lasted for 24 h, and a total of eight samples were collected. Before the sampling, filters were packed in aluminum foil and pretreated by baking in a furnace for 4 h at 450 °C to remove any organic contaminants. The $PM_{2.5}$ concentrations were obtained by weighing the filters before and after exposure on a microbalance (Model BP210D, Sartorius, Göttingen, Germany) with an accuracy of 0.01 mg under a constant temperature of 25 °C and a relative humidity of 50%. Finally, the filter samples were stored in a freezer below −20 °C until further analysis.

2.2. Solid phase extraction methods

2.2.1. Standard solution and aqueous extraction of the aerosol samples

A solution of the SRFA model sample was prepared by dissolving 12 mg of dried solid in 300 mL of ultrapure water and then filtering it through a filter of 0.22 μm pore size. The water-soluble organic fraction of the aerosol sample was obtained with three repetitions of a 30-min ultrasonic extraction with a 220 cm^2 $PM_{2.5}$ filter in 100 mL of ultrapure water. Prior to the extraction, the $PM_{2.5}$ filter was presoaked in ultrapure water for 1 h. The water extracts were then filtered through a membrane filter (0.22 μm pore size) to remove the filter debris and suspended insoluble particles. Finally, approximately 100 mL of water-soluble organic compounds were obtained from each sample.

2.2.2. Isolation procedure

Three one-step SPE isolation procedures were tested for isolation of SRFA and atmospheric HULIS. These procedures were referred to as HLB-M, HLB-N, and PPL, and the details of the procedures are shown in Fig. S1 and the Supporting Information (SI) (Baduel et al., 2009; Fan et al., 2012; Perminova et al., 2014; Varga et al., 2001). The SPE procedure was performed using Waters Oasis HLB (Waters Oasis HLB, 500 mg/6 mL, USA) and Agilent PPL cartridges (Agilent Bond Elut-PPL, 500 mg/6 mL, USA), which consisted of divinylbenzene and N-vinylpyrrolidone reverse-phase sorbent resin and styrene-divinylbenzene copolymer sorbent resin, respectively. All the results were blank corrected by subtracting the filter blank. The data in this study were presented as a mean ± standard deviation based on quadruplicate analyses of the SRFA or WSOC solution of the WS1 aerosol sample (WS1 WSOC).

2.3. Characterization

2.3.1. TOC and UV–Vis measurements

The carbon content of the WSOC and HULIS was determined with a TOC analyzer (Shimadzu, Kyoto, Japan), based on the high-temperature catalytic oxidation method. The data reported here are the average results of three measurements. The UV–Vis spectra of the WSOC and HULIS samples were measured using a UV–visible spectrophotometer (Lambda 850: PerkinElmer, Waltham, MA, USA) and were recorded in the range of 200–700 nm at 1 nm wavelength step sizes. Each spectrum was corrected against a reference cuvette containing pure water.

2.3.2. Optical properties of the HULIS

To characterize the optical properties of the HULIS isolated by the different methods, some spectroscopic parameters were calculated. The specific UV–Vis absorbance at 254 nm was obtained by equation (1) (Fan et al., 2012):

$$SUVA_{254} = A/bc \quad (1)$$

where $SUVA_{254}$ is the specific UV–Vis absorbance at 254 nm (m^2/gC), A is the absorbance at 254 nm, b (m) is the cell path length, and c (mgC/L) is the concentration of the WSOC or HULIS solution.

The absorption Ångström exponent (AAE), which describes the spectral dependence of the light absorption of chromophores in HULIS, was calculated according to the following power law equation (Wu et al., 2018):

$$A_\lambda = K\lambda^{-AAE} \quad (2)$$

where A_λ is the absorbance derived from the spectrophotometer at a given wavelength λ (330–400 nm) and K is a constant.

The mass absorption efficiency (MAE) is a key parameter used to characterize the light absorbing ability of chromophores in HULIS. Based on the light-absorption spectra, the mass absorption efficiency (MAE_{365}, m^2/gC) at a given wavelength (365 nm) of the HULIS in the extracts was calculated (Chen et al., 2016).

$$MAE_{365} = A_{365}/(C \cdot L) \times \ln(10) \quad (3)$$

where A_{365} is the absorbance at 365 nm, C is the concentration of HULIS in solution (μgC mL^{-1}), and L is the absorbing path length.

2.3.3. Proton nuclear magnetic resonance spectroscopy

Approximately 10 mg of dried HULIS from the WS1 sample was dissolved in 500 μL D_2O and then was transferred to a 5-mm NMR tube. The ^1H NMR spectra were obtained at a frequency of 400 MHz on a spectrometer (Avance III 400, Bruker Daltonik GmbH, Bremen, Germany). Data were acquired from 100 scans, with a recycle time of 2 s for a condensed water sample. The length of the proton 90° pulse was 8.87 μs A 1.0 Hz line-broadening weighting function and baseline correction were applied. The identification of the functional groups in the NMR spectra was based on their chemical shift (δH) relative to that of tetramethylsilane (TMS: 0 ppm).

2.3.4. Fourier transform ion cyclotron resonance mass spectrometry analysis

The HULIS fractions isolated from the WS1 sample were analyzed with a 9.4 T SolariX XR FT-ICR MS (Bruker Daltonik) and were ionized in negative ion mode using an ESI ion source. The dried HULIS samples were redissolved in 1 mL of methanol and injected into an electrospray source at a flow rate of 120 mL/h, with a nebulizer gas pressure of 138 kPa and a drying gas pressure of 103 kPa. The ion accumulation time was set to 0.65 s. A total of 100 continuous 4 M data FT-ICR transients were added to enhance the signal-to-noise ratio and the dynamic range. The detection mass range was set to m/z 150–1000 u. The mass spectra were calibrated externally with arginine clusters using a linear calibration. The final spectrum was internally recalibrated with typical O_5-class species peaks using a quadratic calibration in DataAnalysis 4.4 (Bruker Daltonic). The elemental formulas were calculated for each peak in batch mode using custom software, with a signal-to-noise ratio above 10 and a mass tolerance of ±1.5 ppm.

3. Results and discussion

3.1. Analytical performance

To determine the performances of the HLB-M, HLB-N, and PPL methods, the analytical characteristics, i.e., the recovery yield, reproducibility, and limit of detection (LOD), were determined using SRFA standard solutions (Baduel et al., 2009; Fan et al., 2012). As shown in Table 1, the recovery yield of SRFA by the HLB-N method, as determined by the TOC analysis, was 92 ± 0.3%, which was similar to the values reported in previous studies (Table S2) and much larger than the 43 ± 0.2% achieved using the HLB-M method. The lower recovery for the HLB-M method may be attributed to the irreversible adsorption and/or incomplete elution of the SRFA by this method. The PPL method also gave a high recovery (91 ± 0.3%) of SRFA, indicating that the HLB-N and PPL methods were both excellent for the recovery of SRFA. Comparable results were obtained with the UV254 detection; the HLB-N and PPL methods both gave significantly higher recovery yields (93–94%) than that of the HLB-M method (31%). These results indicated that the HLB-N and PPL methods efficiently recovered the FA from the original SRFA solutions, whereas a large amount of SRFA was retained in the HLB resin when pure methanol was used as the eluent. Note that a consistently high analytical recovery (92 ± 2%) of the HULIS model sample (Humic acid sodium salt standard, Sigma Aldrich) was also achieved using the HLB cartridge with methanol:acetonitrile (1:1, v/v) as the eluent (Kumar et al., 2017, 2018), which was similar to the findings of this study. Therefore, HLB-N, PPL, and HLB-methanol: acetonitrile (1:1, v/v) may be equally effective for HULIS quantification.

The reproducibility, expressed as the relative standard deviation (RSD), was determined at approximately 20 mL of 20 μg C/mL SRFA for each protocol (n = 6). The three methods all had relatively low RSD values, i.e., 0.5% (HLB-M), 0.3% (HLB-N), and 0.3% (PPL), as determined by TOC measurements. Therefore, the reproducibility of these methods were all excellent, enabling the measurement of the HULIS in atmospheric samples.

The LOD was calculated as three standard deviations of the blank value obtained for each procedure for a series of six measurements performed with a sample volume of 20 mL of organic-free water. The average values were approximately 29.2, 31.6, and 19.2 μgC for the HLB-M, HLB-N, and PPL methods, respectively. The LOD of the PPL method was lower than those of the HLB-M and HLB-N methods, indicating that the PPL method may be also suitable for detecting HULIS at a lower abundance in atmospheric samples.

3.2. Quantification of HULIS in atmospheric aerosols

To further compare the SPE methods, we evaluated the three methods with aerosol samples. As shown in Table 1, the HULIS fractions recovered from the WS1 WSOC sample were 50% (HLB-M), 57% (HLB-N), and 55% (PPL), as determined by TOC detection. In the case of UV absorption at 254 nm, the recoveries of the total UV absorption of the WS1 sample were 64% (HLB-M), 78% (HLB-N), and 75% (PPL). Very low RSD values (0.35–0.40%) were observed for the three SPE methods, which again indicated that these three methods had good reproducibility for the measurement of HULIS in atmospheric samples.

The three methods were also used to measure the HULIS content in seven aerosol samples at the WS site. The results in Table 1 show that the HULIS fractions recovered from the seven aerosol samples were 35–49% ($HULIS_{HLB\text{-}M}$), 39–57% ($HULIS_{HLB\text{-}N}$), and 39–56% ($HULIS_{PPL}$), as determined by TOC detection. These results were comparable with the data described in previous studies (Table S2). In the case of UV

Table 1
Recovery efficiencies of the SPE methods for Suwannee river fulvic acid (SRFA) and aerosol samples.

Samples	TOC (%)			UV254(%)		
	$HULIS_{HLB-M}$	$HULIS_{HLB-N}$	$HULIS_{PPL}$	$HULIS_{HLB-M}$	$HULIS_{HLB-N}$	$HULIS_{PPL}$
SRFA	43 ± 0.2	92 ± 0.3	91 ± 0.3	31 ± 0.1	93 ± 0.1	94 ± 0.1
WS1	50 ± 0.2	57 ± 0.2	55 ± 0.2	64 ± 0.1	78 ± 0.2	75 ± 0.2
WS2	44	50	48	59	70	67
WS3	41	46	44	67	75	74
WS4	35	43	39	59	74	69
WS5	35	39	39	64	72	73
WS6	37	44	43	54	69	59
WS7	41	47	45	61	81	75
WS8	49	57	56	65	84	76

absorption at 254 nm, the recovery yields were 54–67% (HLB-M), 69–84% (HLB-N), and 59–76% (PPL) for the seven aerosol samples. There were differences in the HULIS content of the WSOC measured by the different analysis methods depending on the isolation procedure (Fig. S2). The HLB-N and PPL methods both gave slightly higher HULIS yields from the WSOC than did the HLB-M method, which were similarly to the result obtained for the SRFA. These findings indicate that the HLB-N and PPL methods may be preferable for the isolation of HULIS in aerosols.

3.3. Characterization of HULIS isolated by the three methods

3.3.1. UV–vis spectra

The UV–Vis spectra obtained for the HULIS fractions and original WSOC of the WS1 sample are shown in Fig. 1. The UV–Vis spectra of the three HULIS fractions were similar, with all of them decreasing sharply with increasing wavelength. There were some differences identified among the three methods, with the specific absorbance of the HULIS fraction obtained by the HLB-N and PPL methods being slightly higher than that obtained by the HLB-M method in the UV region. These results indicated that more light-absorbing organic constituents were recovered by the HLB-N and PPL methods than by the HLB-M method. The lower light absorption of the $HULIS_{HLB-M}$ was probably related to the retention of some strong light-absorbing compounds in the resin due to irreversible adsorption in the HLB-M protocol. It was therefore concluded that the HULIS fractions isolated by the HLB-N and PPL methods were more representative of the HULIS in ambient aerosols.

The spectroscopic properties (i.e., $SUVA_{254}$, MAE_{365}, and AAE) were determined to elucidate the properties of the HULIS isolated by the different methods. As shown in Table 2, the $SUVA_{254}$ values of the three isolated HULIS fractions ($HULIS_{HLB-M}$, $HULIS_{HLB-N}$ and $HULIS_{PPL}$) were in a small range of 2.3–2.5 L/(mgC·m), which suggested there were similar contents of light-absorbing organic components in the three HULIS fractions. However, the $SUVA_{254}$ values of the three HULIS fractions were all higher than that for the WSOC (1.9 L/(mgC·m)), which indicated that the HULIS isolated by the SPE methods had enriched fraction of light-absorbing organic constituents than did the original WSOC (Fan et al., 2012).

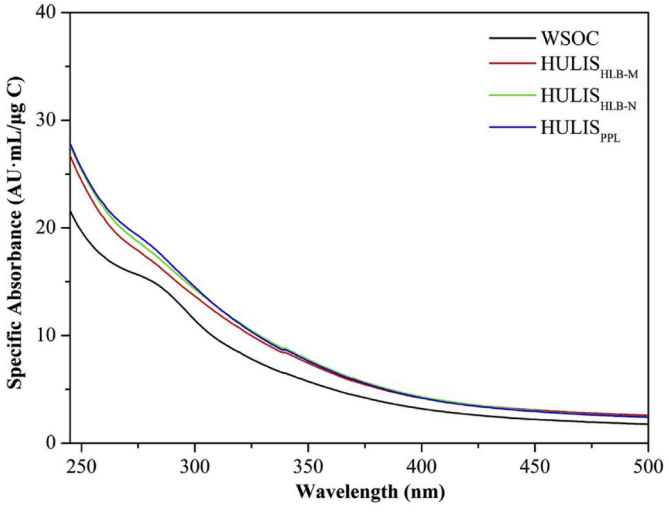

Fig. 1. Comparison of UV spectra of HULIS resulting from the three SPE methods for WS1 sample.

The MAE_{365} and AAE values revealed the light-absorbing properties of the WSOC and HULIS samples (Li et al., 2019; Lin et al., 2017) and were used to evaluate the three SPE methods in the present study. As shown in Table 2, the MAE_{365} values of the three isolated HULIS fractions were in the range of 1.4–1.5 m^2/gC, all higher than the 1.1 m^2/gC of the WSOC, suggesting that all three HULIS fractions had stronger light absorption ability than the original WSOC. However, it is worth noting that light absorption ability of the three HULIS fractions ($HULIS_{HLB-M}$, $HULIS_{HLB-N}$ and $HULIS_{PPL}$) were similar because the MAE_{365} values of the three isolated HULIS fractions were in very small ranges (1.4–1.5 m^2/gC).

The AAE of the HULIS fitted between the wavelengths of 330 and 400 nm for the three HULIS fractions and the WSOC were 4.3, 4.4, 4.4, and 4.3, respectively. The AAE values of the HULIS fraction were in the range of those for ambient HULIS (3.0–8.3) reported in previous studies but with relative lower levels (Cheng et al., 2016; Fan et al., 2016; Hecobian et al., 2010; Kumar et al., 2017; Srinivas et al., 2016). The AAE values of the three HULIS fractions were all similar to those of the original WSOC, indicating that the light-absorbing chromophores in the HULIS fractions isolated by these methods may have been similar to those in the original WSOC.

3.3.2. Proton nuclear magnetic resonance spectroscopy

Fig. 2 shows the ^{1}H-NMR spectra of the isolated HULIS fractions and the original WSOC. The spectra were quite similar and were all characterized by a combination of sharp peaks of the most abundant organic species and convoluted spectral resonances of the organic compounds present at low concentrations. For the sharp signals, a limited number of resonances were assigned to specific organic compounds based on the reference ^{1}H-NMR spectra of model compounds and a comparison with previous studies (Chalbot and Kavouras, 2014; Chalbot et al., 2014; Graham et al., 2002; Suzuki et al., 2001). These sharp signals were assigned to phthalic acid (at δ7.47 ppm) and terephthalic acid (at δ8.01 ppm)], which are associated with both primary and secondary organic aerosols; monomethylamine (at δ2.59 ppm); levoglucosan (at δ3.67 ppm), which is associated with biomass burning emissions; sugars [glucose (at δ3.39–δ3.41 ppm), fructose (at δ3.46 and δ3.55 ppm), and sucrose (at δ3.91–δ4.03 ppm)], and tracers of marine secondary organic aerosol (methanesulfonic acid at δ3.55–δ3.59 ppm).

Although these sharp peaks were identified, most of the signals in the ^{1}H-NMR spectra remained unresolved and appeared as a continuous distribution, suggesting that the HULIS and WSOC fractions mainly consisted of a complex mixture of organic species (Chalbot et al., 2014, 2016; Song et al., 2012). According to the chemical shift assignments of

Table 2
The proton species and corresponding content percentages of WSOC and HULIS for WS1 sample.

Samples	^{1}H NMR (%)				Optical properties		
	H–C (0.6–1.9)	H–C–C= (1.9–3.2)	H–C–O (3.4–4.4)	Ar–H (6.5–8.5)	$SUVA_{254}$ L/(mgC·m)	MAE_{365} m^2/gC	AAE
WSOC	32	30	28	10	1.9	1.1	4.3
$HULIS_{HLB-M}$	41	34	14	11	2.3	1.4	4.3
$HULIS_{HLB-N}$	45	30	13	12	2.4	1.5	4.4
$HULIS_{PPL}$	44	31	13	12	2.5	1.5	4.4

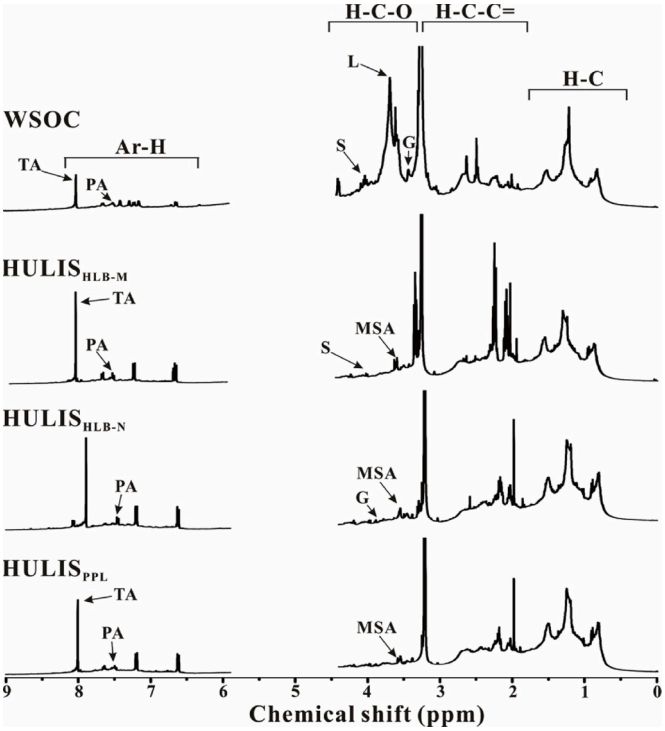

Fig. 2. 400 MHz solution-state ^{1}H NMR spectra of WSOC and HULIS extracted from WS1 sample. Four spectral regions are identified at the top of the spectra: H–C, H–C═C, H–C–O, and Ar–H. The peaks were assigned to specific compounds as follows: levoglucosan (L), glucose (G), sucrose (S), methanesulfonate (MSA), phthalic acid (PA), terephthalic acid (TA).

the proton resonance spectra, four categories of H functional groups were assigned and integrated in the spectra: (1) H–C (0.6–1.9 ppm): aliphatic protons in alkyl chains, which included protons from methyl ($R–CH_3$), methylene ($R–CH_2$), and methyne (R–CH) groups; (2) H–C–C= (1.9–3.2 ppm): aliphatic protons attached to carbon atoms adjacent to carbonyl (H–C–C═O) or imino (H–C–C═N) groups or aromatic rings. (3) H–C–O (3.4–4.4 ppm): protons on carbon atoms singly bound to oxygen atoms in alcohols, polyols, ethers, and esters, indicating that carbohydrates and ethers were present in the HULIS; and (4) Ar–H (6.5–8.5 ppm): aromatic protons. Among these functional groups, the wide range of chemical shifts of the signals attributed to aromatic protons suggested the occurrence of highly substituted aromatic rings, e.g., phenols, alkylbenzenes, benzoic acids, or esters.

To further evaluate the ^{1}H NMR data, the abundances of the four categories of structural units were estimated by the integration of each spectral region. As shown in Table 2, the isolated HULIS and original WSOC exhibited similar patterns in terms of their structural characteristics. They were characterized by a relatively high H–C (32–45%) and H–C═C content (30–34%), moderate H–C–O content (13–28%), and a relatively low Ar–H content (10–12%). These four functional groups have also been detected in the ^{1}H NMR spectra of atmospheric HULIS in other studies, and the distributions of the H functional groups were comparable with the data for WSOC and HULIS in atmospheric samples (Chalbot et al., 2016; Decesari et al., 2007; Graham et al., 2002; Kumar et al., 2017; Lopes et al., 2015; Song et al., 2012).

As shown in Fig. 2, there were some differences between the isolated HULIS fractions and original WSOC. Relatively high amounts of oxygenated aliphatic protons were observed in the WSOC, but they were absent or present in low amounts in the three HULIS fractions. This observation was reasonable because high polarity oxygenated aliphatic components are not retained by SPE cartridges (Baduel et al., 2009; Fan et al., 2012; Lin et al., 2010). For example, there were sharp signals at δ3.67 ppm in the WSOC spectrum, suggesting that a large amount of levoglucosan was present (Chalbot et al., 2016; Decesari et al., 2000). This sharp peak was not present in the corresponding region of the HULIS spectra. Some distinct peaks were observed in the 6.5–8.5 ppm region in the HULIS spectra, but they were slightly weaker in the WSOC spectrum, suggesting that the HULIS isolated by the three SPE methods contained more aromatic structures from the WSOC. As shown in Table 2, these differences were also indicated by the relative contents of the different functional groups, and, compared with the WSOC, the three HULIS fractions all contained a relatively higher Ar–H content and lower H–C–O content.

Furthermore, some differences were observed among the three HULIS fractions isolated by the different methods. The $HULIS_{HLB-N}$ had a functional distribution similar to that of the $HULIS_{PPL}$ (Table 2), and both were characterized by higher levels of aliphatic C–H groups and lower levels of unsaturated aliphatic protons than those of the $HULIS_{HLB-M}$. Moreover, the sum of the aliphatic and aromatic C–H in the $HULIS_{HLB-N}$ and $HULIS_{PPL}$ fractions (56%–57%) was higher than that in the $HULIS_{HLB-M}$ fraction (52%), which indicated that relative higher content of the weak polar organic species (aliphatic and aromatic C–H) in HULIS fractions isolated by the HLB-N and PPL methods than those isolated by the HLB-M method. These organic compounds cannot be fully eluted by pure methanol because of their strong bonds with HLB resin. Compared with the $HULIS_{PPL}$, the $HULIS_{HLB-N}$ had unique properties. For example, a distinct chemical shift of the aromatic band at δ7.8 ppm, which was observed only in the $HULIS_{HLB-N}$ spectra, corresponded to the presence of aromatic amine or amino groups. These observations were consistent with those of a previous study (Fan et al., 2013). These differences may suggest the formation of aromatic rings carrying more electron-donor groups, such as the amino group possibly formed during the solvent treatment (2% ammonia/methanol) (Decesari et al., 2000; Suzuki et al., 2001), which may also suggest that the PPL method was more advantageous than the HLB-N method for extracting HULIS from ambient aerosols.

3.3.3. *Fourier transform ion cyclotron resonance mass spectrometry*

The molecular characteristics of the HULIS isolated by the three methods were investigated with FT-ICR MS. As shown in Fig. 3, thousands of peaks were observed in the spectra in the mass range between 150 and 600 m/z. High intensity ions were located between 200 and 400 m/z and were comparable with those reported for WSOC (i.e., HULIS) in atmospheric aerosols (Lin et al., 2012; Song et al., 2018). Based on the molecular formulae identified in the FT-ICR mass spectra, four main groups of compounds were identified: C, H, and O only (CHO), N-containing compounds (CHON), S-containing compounds (CHOS),

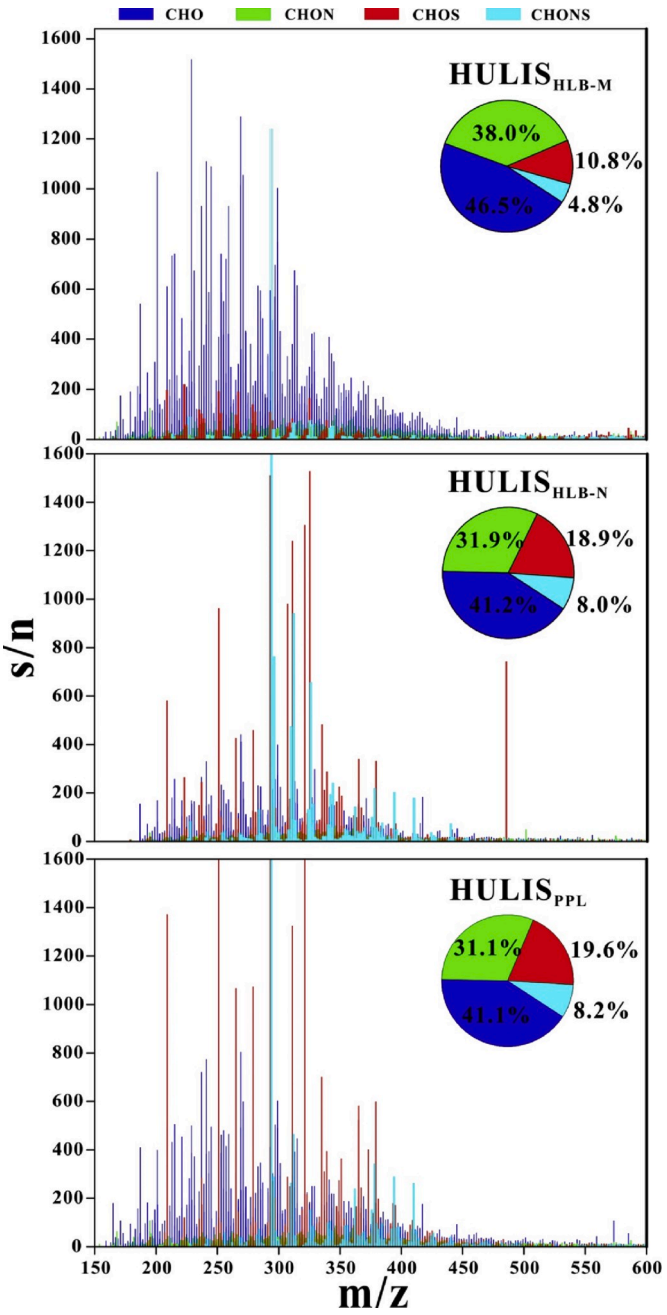

Fig. 3. The reconstructed Fourier-transform ion cyclotron resonance (FT-ICR) mass spectra for $HULIS_{HLB-M}$, $HULIS_{HLB-N}$, and $HULIS_{PPL}$ fractions extracted from WS1 sample. The pie charts of the percentages of CHO, CHON, CHOS, and CHONS formula groups are also presented.

and N- and S-containing compounds (CHONS). As shown in Fig. 3, the three HULIS fractions had similar distributions of the four groups among their total molecules. The CHO group was typically present in the highest abundance (41–47%) among all the molecules, followed by the CHON group (31–38%), while the CHOS and CHONS groups were present at relatively low contents of 11–20% and 4.8–8.2%, respectively. This distribution of molecular formulae was consistent with those of other ambient aerosol and biomass burning samples (Song et al., 2018; Willoughby et al., 2014).

There were some differences in the distributions of these groups among the three HULIS fractions. As shown in Fig. 3, the $HULIS_{HLB-N}$ and $HULIS_{PPL}$ had very similar compositions, which were characterized by a higher content of S-containing compounds (CHOS and CHONS) and a lower content of CHO and CHON compounds than that of the $HULIS_{HLB-M}$. Thus, the HULIS fractions isolated with the HLB-N and PPL methods had similar molecular compositions and contained a relatively high content of S-containing compounds. In addition, a substantial amount of S-containing compound was retained by the HLB resin when methanol was used as the eluent.

Table 3 presents the number of formulae in each compound category and the relative-abundance weighted values of the molecular weight (MW), elemental ratios, double bond equivalents (DBEs), modified aromaticity index (AI_{mod}), and carbon oxidation state (OS_C) for the three HULIS samples. The $HULIS_{PPL}$ and $HULIS_{HLB-N}$ samples had similar molecular properties, such as the H/C_w, O/C_w, and N/C_w ratios and DBE/C_w, $AI_{mod,w}$, and $OS_{C,w}$ values, indicating that they may have had similar molecular characteristics. As shown in Table 3, some differences were identified between the two HULIS fractions ($HULIS_{PPL}$ and $HULIS_{HLB-N}$) and $HULIS_{HLB-M}$. The $HULIS_{PPL}$ and $HULIS_{HLB-N}$ had lower weighted $AI_{mod,w}$ and DBE/C_w values than did the $HULIS_{HLB-M}$, and, therefore, the $HULIS_{PPL}$ and $HULIS_{HLB-N}$ fractions may have contained a relatively small amount of aromatic components (Koch and Dittmar, 2006). In addition, the $HULIS_{PPL}$ and $HULIS_{HLB-N}$ had a higher S/C_w ratio and lower $OS_{C,w}$ values than those of the $HULIS_{HLB-M}$. These results indicated that the irreversible OC fractions retained by the HLB-M method consisted mainly of relatively hydrophobic components, with low levels of aromatic species and high levels of organic species with a high degree of oxidation. The relatively low content of aromatic species was inconsistent with the results obtained from the ^{1}H NMR spectra, which may have been due to the limitations of FT-ICR MS in the detection of elemental compositions. Only polar compounds could be detected by the ESI source, whereas the proton functional groups identified by the ^{1}H NMR spectra enabled the total molecular structure to be identified.

For a further comparison of the molecular characteristics of the HULIS fractions isolated by the different methods and to explore the impact of sorption selectivity on the molecular composition of the HULIS isolates, we analyzed the molecular properties of each compound group in the HULIS fractions based on the AI_{mod} values (Koch and Dittmar, 2006). The molecules were divided into aliphatic ($AI = 0$), olefinic ($0 < AI < 0.5$), aromatic ($0.5 \leq AI < 0.67$), and condensate aromatic ($AI \geq 0.67$) classes. As shown in Fig. 3, the CHO group was predominant in all the three HULIS fractions, and the CHO groups in the different HULIS fractions were present with very similar H/C_w, O/C_w, and OM/OC_w ratios and DBE_w, DBE/C_w, and $AI_{mod,w}$ values (Table 3). Furthermore, the relative contents of aliphatic, olefinic, aromatic, and condensed aromatic species in the three CHO groups were very similar (Table S3). These results indicated that the CHO species in the HULIS isolated by the different methods had similar chemical and elemental compositions. However, some differences were identified, with the $OS_{C,w}$ values of the $HULIS_{PPL}$ and $HULIS_{HLB-N}$ being slightly lower than that of the $HULIS_{HLB-M}$, which may have indicated that more of the less polar compounds were recovered by the HLB-N and PPL methods.

As shown in Fig. 4, the CHON formulas in the three HULIS fractions were localized in similar regions, with an O/C ratio in the range of 0.1–1.0 and H/C ratio in the range of 0.3–1.8. The fractions also had similar molecular properties, such as the H/C_w, N/C_w, and DBE/C_w ratios and $AI_{mod,w}$ values. However, some differences were identified among the three HULIS fractions. For example, the $HULIS_{HLB-M}$ and $HULIS_{PPL}$ were extremely similar, with higher O/C_w ratios and $OS_{C,w}$ values than those of the $HULIS_{HLB-N}$, indicating that the CHON compounds among the $HULIS_{HLB-N}$ compounds were less oxidized than those of the $HULIS_{HLB-M}$ and $HULIS_{PPL}$. These differences were consistent with the relatively high abundances of CHON compounds with high O/N ratios, as shown in Fig. S3, in which more high O/N ratio subgroups were identified in the CHON compounds of the $HULIS_{HLB-M}$ and $HULIS_{PPL}$. Moreover, the $HULIS_{HLB-N}$ contained more olefinic groups and fewer aliphatic and condensed aromatic groups than did the $HULIS_{HLB-M}$ and $HULIS_{PPL}$ fractions (Table S3). These differences suggested that the

Table 3
Number of formulas in each compound category and the average values of elemental ratios, molecular weight, double-bond equivalents (DBEs), aromaticity index (AI_{mod}) and carbon oxidation state (OS_C).

Samples	Elemental compositions	Number of formulas	MW_w	H/C_w	O/C_w	N/C_w	S/C_w	O/N_w	O/S_w	OM/OC_w	DBE_w	DBE/C_w	$AI_{mod,w}$	$OS_{C,w}$
$HULIS_{HLB-M}$	CHO-	1263	305	1.3	0.43	–	–	–	–	1.7	5.9	0.39	0.27	−0.44
	CHON-	1033	345	1.1	0.48	0.08	–	6.8	–	1.8	8.5	0.50	0.37	−0.38
	CHOS-	293	346	1.6	0.49	–	0.08	–	6.3	2.0	4.5	0.24	0.09	−0.78
	CHONS-	130	371	1.5	0.66	0.09	0.09	7.6	7.6	2.3	5.5	0.32	0.32	−0.63
	all in ESI-	2719	315	1.3	0.45	0.01	0.01	1.3	0.5	1.7	6.3	0.40	0.28	−0.45
$HULIS_{HLB-N}$	CHO-	986	316	1.3	0.39	–	–	–	–	1.6	6.0	0.37	0.26	−0.52
	CHON-	762	345	1.2	0.44	0.07	–	6.5	–	1.8	8.3	0.49	0.38	−0.53
	CHOS-	453	328	1.7	0.42	–	0.07	–	5.9	1.9	2.8	0.18	0.05	−1.0
	CHONS-	191	340	1.6	0.79	0.10	0.10	8.5	8.5	2.6	3.0	0.27	0.08	−0.52
	all in ESI-	2392	326	1.4	0.44	0.02	0.03	1.8	2.5	1.8	5.1	0.32	0.19	−0.64
$HULIS_{PPL}$	CHO-	1336	320	1.3	0.41	–	–	–	–	1.7	6.3	0.39	0.27	−0.48
	CHON-	1010	353	1.1	0.47	0.07	–	7.0	–	1.8	8.5	0.50	0.38	−0.37
	CHOS-	635	335	1.7	0.43	–	0.07	–	6.1	1.9	2.7	0.17	0.04	−0.98
	CHONS-	267	375	1.6	0.70	0.08	0.08	8.6	8.6	2.3	3.9	0.26	0.04	−0.60
	all in ESI-	3248	332	1.4	0.44	0.01	0.02	1.5	2.2	1.8	5.5	0.34	0.21	−0.59

molecular composition of the $HULIS_{HLB-N}$ may have been transformed during treatment by the HLB-N method.

The CHOS compounds were identified in every HULIS fraction but were more prevalent in the $HULIS_{HLB-N}$ and $HULIS_{PPL}$ fractions than in the $HULIS_{HLB-M}$. Most (94%) of these compounds had O/S ratios of at least 4, indicating that they were mostly sulfate (-OSO_3H) or sulfonate groups (-SO_3). Furthermore, some differences in the elemental compositions and molecular structures were observed among the three HULIS fractions. As shown in Table 3, the CHOS compounds in the $HULIS_{HLB-N}$ were very similar to those in the $HULIS_{PPL}$, and they both had lower O/C_w ratios and DBE_w, DBE/C_w, and AI_{mod} values than those of the $HULIS_{HLB-M}$. Moreover, relatively low amounts of aromatic compounds were observed for the CHOS groups in the $HULIS_{HLB-N}$ and $HULIS_{PPL}$ (Table S3). Therefore, the irreversible CHOS fractions obtained by the HLB-M method consisted mainly of low aromaticity compounds with low O contents.

There were also more CHONS compounds in the $HULIS_{HLB-N}$ and $HULIS_{PPL}$ fractions than in the $HULIS_{HLB-M}$, and their molecular structures also clearly differed. As shown in Table 3, the $HULIS_{PPL}$ and $HULIS_{HLB-N}$ fractions had higher O/S_w ratios and lower DBE/C_w and $AI_{mod,w}$ values than those of the $HULIS_{HLB-M}$. These differences may have been due to the introduction of some irreversible OC in the HLB resin when methanol was used as the eluant. Moreover, the $HULIS_{HLB-N}$ and $HULIS_{PPL}$ contained more aliphatic and aromatic groups and fewer olefinic groups than did the $HULIS_{HLB-M}$ (Table S3). In addition, some differences were observed between the $HULIS_{HLB-N}$ and $HULIS_{PPL}$, with $HULIS_{HLB-N}$ having a lower MW as well as containing fewer olefinic groups, which may have been due to the alkaline hydrolysis of some of the molecules of the HULIS.

4. Conclusion

In this study, the HLB-M, HLB-N, and PPL methods were compared using SRFA and ambient aerosols, and the following conclusions were obtained:

(1) The HLB-N and PPL methods were found to have a high yields, good reproducibility, and low LOD for SRFA and HULIS, indicating that these two methods were reliable for the quantification of low levels of ambient HULIS. The relatively lower isolation yield of the HLB-M method may have indicated that some light-absorbing compounds remained in the HLB resin during the HLB-M treatment.
(2) The three SPE methods were all suitable for the isolation of high UV absorbance aromatic compounds; however, there were differences in the chemical structures and molecular compositions of the HULIS isolated by the three methods. The $HULIS_{HLB-N}$ and $HULIS_{PPL}$ were both characterized by more aliphatic C–H groups and fewer unsaturated aliphatic protons than those of the $HULIS_{HLB-M}$, indicating that relative higher content of the weak polar organic species in HULIS fractions isolated by the HLB-N and PPL methods than those isolated by the HLB-M method. The $HULIS_{HLB-N}$ and $HULIS_{PPL}$ fractions had similar molecular compositions, which were characterized by a higher content of S-containing compounds (CHOS and CHONS) and lower content of CHO and CHON compounds than those of the $HULIS_{HLB-M}$. Furthermore, the $HULIS_{PPL}$ and $HULIS_{HLB-N}$ had a lower $AI_{mod,w}$ and higher S/C ratio than those of the $HULIS_{HLB-M}$. Therefore, it can be concluded that the $HULIS_{PPL}$ and $HULIS_{HLB-N}$ fractions contained relatively low amounts of aromatic components but substantial amounts of S-containing compounds. It was also found that the molecular composition of the $HULIS_{HLB-N}$ may have undergone a chemical transformation during treatment with the HLB-N method. Therefore, caution should be exercised when using the HLB-N method for the characterization of HULIS in atmospheric aerosols.

The PPL method had many advantages, such as a high recovery yield, good reproducibility, and low LOD, and the properties of the HULIS extracted by this process were not changed during the treatment and were more representative of the global matrix. Therefore, we can conclude that the PPL method serves equally good as compared to other two methods, and one can utilize PPL method also for HULIS isolation and characterization.

However, in the present study, only one type of aerosol sample was tested for the chemical and molecular composition of the HULIS isolated by the different methods. Therefore, further efforts will be required to comparatively study the HULIS isolation methods, possibly using more types of aerosol samples collected from different environments or sources and from aerosol samples collected in different seasons.

Declaration of competing interest

The authors declare that they have no known competing financial interests or personal relationships that could have appeared to influence the work reported in this paper.

CRediT authorship contribution statement

Chunlin Zou: Formal analysis, Writing - original draft. **Meiju Li:**

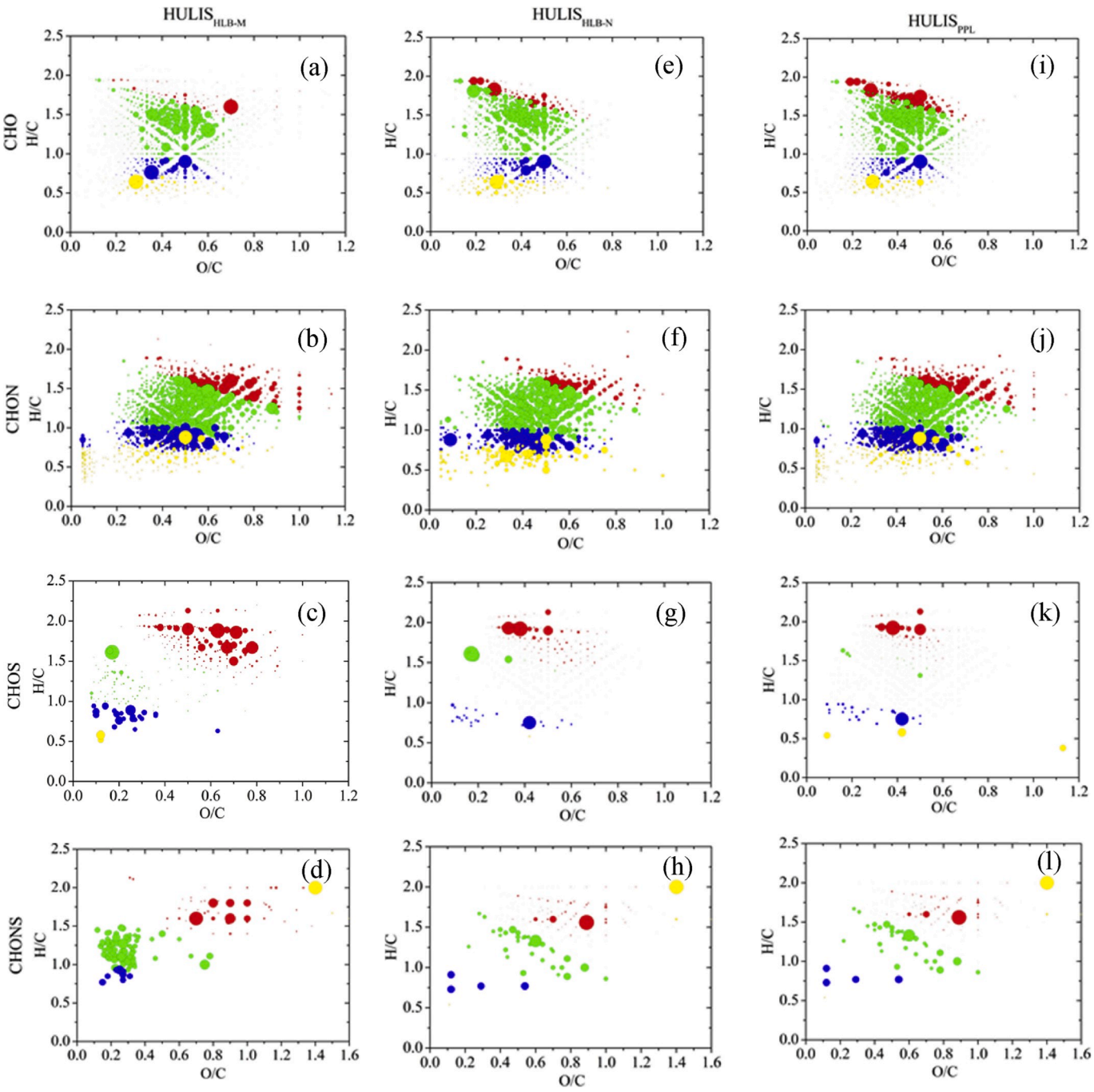

Fig. 4. Van Krevelen diagrams of elemental H/C and O/C ratios for molecular formulas assigned to the (a–d) HULIS$_{HLB-M}$, (e–h) HULIS$_{HLB-N}$, and (i–l) HULIS$_{PPL}$. Each diagram is plotted based on elemental content of each molecular formula (CHO, CHON, CHOS, and CHONS). Formulae with red, green, blue, and yellow are aliphatic, olefinic, aromatic, and condensed aromatic correspond to their aromaticity based on AI$_{mod}$, respectively. (For interpretation of the references to colour in this figure legend, the reader is referred to the Web version of this article.)

Formal analysis. **Tao Cao:** Formal analysis. **Mengbo Zhu:** Formal analysis. **Xingjun Fan:** Writing - review & editing, Formal analysis. **Shiyun Peng:** Writing - review & editing. **Jianzhong Song:** Project administration, Writing - original draft. **Bin Jiang:** Formal analysis. **Wanglu Jia:** Writing - review & editing. **Chiling Yu:** Formal analysis. **Haiyan Song:** Formal analysis. **Zhiqiang Yu:** Writing - review & editing. **Jun Li:** Writing - review & editing. **Gan Zhang:** Writing - review & editing. **Ping'an Peng:** Writing - review & editing.

Acknowledgments

This study was supported by the Natural Science Foundation of China (Grants No. 41673117, 41977188, and 41473104), State Key Laboratory of Organic Geochemistry (GIGCAS) (Grant No. SKLOG2016-A08), and Guangdong Foundation for Program of Science and Technology Research (Grant No. 2017B030314057). We greatly appreciate the assistance of two anonymous reviewers for the helpful comments that greatly improved the quality of this manuscript. This is contribution No. IS-2821 from GIGCAS.

Appendix A. Supplementary data

Supplementary data to this article can be found online at https://doi.org/10.1016/j.atmosenv.2020.117370.

References

Baduel, C., Voisin, D., Jaffrezo, J.L., 2009. Comparison of analytical methods for Humic like Substances (HULIS) measurements in atmospheric particles. Atmos. Chem. Phys. 9, 5949–5962.

Chalbot, M.C.G., Kavouras, I.G., 2014. Nuclear magnetic resonance spectroscopy for determining the functional content of organic aerosols: a review. Environ. Pollut. 191, 232–249.

Chalbot, M.G., Brown, J., Chitranshi, P., da Costa, G.G., Pollock, E.D., Kavouras, I.G., 2014. Functional characterization of the water-soluble organic carbon of size-fractionated aerosol in the southern Mississippi Valley. Atmos. Chem. Phys. 14, 6075–6088.

Chalbot, M.G., Chitranshi, P., da Costa, G.G., Pollock, E., Kavouras, I.G., 2016. Characterization of water-soluble organic matter in urban aerosol by ^{1}H-NMR spectroscopy. Atmos. Environ. 128, 235–245.

Chen, Q.C., Ikemori, F., Mochida, M., 2016. Light absorption and excitation-emission fluorescence of urban organic aerosol components and their relationship to chemical structure. Environ. Sci. Technol. 50, 10859–10868.

Cheng, Y., Engling, G., Moosmaller, H., Arnott, W.P., Chen, L.W.A., Wold, C.E., Hao, W. M., He, K.B., 2016. Light absorption by biomass burning source emissions. Atmos. Environ. 127, 347–354.

Decesari, S., Facchini, M.C., Fuzzi, S., Tagliavini, E., 2000. Characterization of water-soluble organic compounds in atmospheric aerosol: a new approach. J. Geophys. Res. Atmos. 105, 1481–1489.

Decesari, S., Mircea, M., Cavalli, F., Fuzzi, S., Moretti, F., Tagliavini, E., Facchini, M.C., 2007. Source attribution of water-soluble organic aerosol by nuclear magnetic resonance spectroscopy. Environ. Sci. Technol. 41, 2479–2484.

Dinar, E., Taraniuk, I., Graber, E.R., Katsman, S., Moise, T., Anttila, T., Mentel, T.F., Rudich, Y., 2006. Cloud condensation nuclei properties of model and atmospheric HULIS. Atmos. Chem. Phys. 6, 2465–2482.

Dittmar, T., Koch, B., Hertkorn, N., Kattner, G., 2008. A simple and efficient method for the solid-phase extraction of dissolved organic matter (SPE-DOM) from seawater. Limnol Oceanogr. Methods 6, 230–235.

Duarte, R.M.B.O., Santos, E.B.H., Pio, C.A., Duarte, A.C., 2007. Comparison of structural features of water-soluble organic matter from atmospheric aerosols with those of aquatic humic substances. Atmos. Environ. 41, 8100–8113.

Fan, X., Song, J., Peng, P., 2013. Comparative study for separation of atmospheric humic-like substance (HULIS) by ENVI-18, HLB, XAD-8 and DEAE sorbents: elemental composition, FT-IR, 1H-NMR and off-line thermochemolysis with tetramethylammonium hydroxide (TMAH). Chemosphere 93, 1710–1719.

Fan, X., Song, J., Peng, P.a., 2012. Comparison of isolation and quantification methods to measure humic-like substances (HULIS) in atmospheric particles. Atmos. Environ. 60, 366–374.

Fan, X.J., Wei, S.Y., Zhu, M.B., Song, J.Z., Peng, P.A., 2016. Comprehensive characterization of humic-like substances in smoke PM2.5 emitted from the combustion of biomass materials and fossil fuels. Atmos. Chem. Phys. 16, 13321–13340.

Graber, Rudich, 2006. Atmospheric HULIS: how humic-like are they? A comprehensive and critical review. Atmos. Chem. Phys. 6, 729–753.

Graham, B., Mayol-Bracero, O.L., Guyon, P., Roberts, G.C., Decesari, S., Facchini, M.C., Artaxo, P., Maenhaut, W., Koll, P., Andreae, M.O., 2002. Water-soluble organic compounds in biomass burning aerosols over Amazonia - 1. Characterization by NMR and GC-MS. J. Geophys. Res. Atmos. 107 https://doi.org/10.1029/2001JD000336.

Green, N.W., Perdue, E.M., Aiken, G.R., Butler, K.D., Chen, H., Dittmar, T., Niggemann, J., Stubbins, A., 2014. An intercomparison of three methods for the large-scale isolation of oceanic dissolved organic matter. Mar. Chem. 161, 14–19.

Hecobian, A., Zhang, X., Zheng, M., Frank, N., Edgerton, E.S., Weber, R.J., 2010. Water-Soluble Organic Aerosol material and the light-absorption characteristics of aqueous extracts measured over the Southeastern United States. Atmos. Chem. Phys. 10, 5965–5977.

Koch, B.P., Dittmar, T., 2006. From mass to structure: an aromaticity index for high-resolution mass data of natural organic matter. Rapid Commun. Mass Spectrom. 20, 926–932.

Kumar, V., Goel, A., Rajput, P., 2017. Compositional and surface characterization of HULIS by UV-Vis, FTIR, NMR and XPS: wintertime study in Northern India. Atmos. Environ. 164, 468–475.

Kumar, V., Rajput, P., Goel, A., 2018. Atmospheric abundance of HULIS during wintertime in Indo-Gangetic Plain: impact of biomass burning emissions. J. Atmos. Chem. 75, 385–398.

Li, M., Fan, X., Zhu, M., Zou, C., Song, J., Wei, S., Jia, W., Peng, P., 2019. Abundance and light absorption properties of brown carbon emitted from residential coal combustion in China. Environ. Sci. Technol. 53, 595–603.

Li, Y., Harir, M., Uhl, J., Kanawati, B., Lucio, M., Smirnov, K.S., Koch, B.P., Schmitt-Kopplin, P., Hertkorn, N., 2017. How representative are dissolved organic matter (DOM) extracts? A comprehensive study of sorbent selectivity for DOM isolation. Water Res. 116, 316–323.

Lin, P., Bluvshtein, N., Rudich, Y., Nizkorodov, S.A., Laskin, J., Laskin, A., 2017. Molecular chemistry of atmospheric brown carbon inferred from a nationwide biomass burning event. Environ. Sci. Technol. 51, 11561–11570.

Lin, P., Huang, X.-F., He, L.-Y., Zhen Yu, J., 2010. Abundance and size distribution of HULIS in ambient aerosols at a rural site in South China. J. Aerosol Sci. 41, 74–87.

Lin, P., Rincon, A.G., Kalberer, M., Yu, J.Z., 2012. Elemental composition of HULIS in the Pearl River Delta Region, China: results inferred from positive and negative electrospray high resolution mass spectrometric data. Environ. Sci. Technol. 46, 7454–7462.

Lopes, S.P., Matos, J.T.V., Silva, A.M.S., Duarte, A.C., Duarte, R.M.B.O., 2015. 1H-NMR studies of water- and alkaline-soluble organic matter from fine urban atmospheric aerosols. Atmos. Environ. 119, 374–380.

Park, S.S., Yu, J., 2016. Chemical and light absorption properties of humic-like substances from biomass burning emissions under controlled combustion experiments. Atmos. Environ. 136, 114–122.

Perminova, I.V., Dubinenkov, I.V., Kononikhin, A.S., Konstantinov, A.I., Zherebker, A.Y., Andzhushev, M.A., Lebedev, V.A., Bulygina, E., Holmes, R.M., Kostyukevich, Y.I., Popov, I.A., Nikolaev, E.N., 2014. Molecular mapping of sorbent selectivities with respect to isolation of Arctic dissolved organic matter as measured by Fourier transform mass spectrometry. Environ. Sci. Technol. 48, 7461–7468.

Samburova, Zenobi, Kalberer, M., 2005. Characterization of high molecular weight compounds in urban atmospheric particles. Atmos. Chem. Phys. 5, 2163–2170.

Song, J., He, L., Peng, P.a., Zhao, J., Ma, S., 2012. Chemical and isotopic composition of humic-like substances (HULIS) in ambient aerosols in Guangzhou, South China. Aerosol. Sci. Technol. 46, 533–546.

Song, J., Li, M., Jiang, B., Wei, S., Fan, X., Peng, P., 2018. Molecular characterization of water-soluble humic like substances in smoke particles emitted from combustion of biomass materials and coal using Ultrahigh-resolution electrospray ionization fourier transform ion cyclotron resonance mass spectrometry. Environ. Sci. Technol. 52, 2575–2585.

Srinivas, B., Rastogi, N., Sarin, M.M., Singh, A., Singh, D., 2016. Mass absorption efficiency of light absorbing organic aerosols from source region of paddy-residue burning emissions in the Indo-Gangetic Plain. Atmos. Environ. 125, 360–370.

Stubbins, A., Hood, E., Raymond, P.A., Aiken, G.R., Sleighter, R.L., Hernes, P.J., Butman, D., Hatcher, P.G., Striegl, R.G., Schuster, P., Abdulla, H.A.N., Vermilyea, A. W., Scott, D.T., Spencer, R.G.M., 2012. Anthropogenic aerosols as a source of ancient dissolved organic matter in glaciers. Nat. Geosci. 5, 198–201.

Sullivan, A.P., Weber, R.J., 2006. Chemical characterization of the ambient organic aerosol soluble in water: 1. Isolation of hydrophobic and hydrophilic fractions with a XAD-8 resin. J. Geophys. Res. Atmos. 111 https://doi.org/10.1029/2005JD006485.

Suzuki, Y., Kawakami, M., Akasaka, K., 2001. ^{1}H-NMR application for characterizing water-soluble organic compounds in urban atmospheric particles. Environ. Sci. Technol. 35, 2656–2664.

Varga, B., Kiss, G., Ganszky, I., Gelencser, A., Krivacsy, Z., 2001. Isolation of water-soluble organic matter from atmospheric aerosol. Talanta 55, 561–572.

Verma, V., Fang, T., Xu, L., Peltier, R.E., Russell, A.G., Ng, N.L., Weber, R.J., 2015. Organic aerosols associated with the generation of reactive oxygen species (ROS) by water-soluble $PM_{2.5}$. Environ. Sci. Technol. 49, 4646–4656.

Verma, V., Rico-Martinez, R., Kotra, N., King, L., Liu, J., Snell, T.W., Weber, R.J., 2012. Contribution of water-soluble and insoluble components and their hydrophobic/hydrophilic subfractions to the reactive oxygen species-generating potential of fine ambient aerosols. Environ. Sci. Technol. 46, 11384–11392.

Wang, B., Knopf, D.A., 2011. Heterogeneous ice nucleation on particles composed of humic-like substances impacted by O_3. J. Geophys. Res. Atmos. 116 https://doi.org/10.1029/2010JD014964.

Willoughby, A.S., Wozniak, A.S., Hatcher, P.G., 2014. A molecular-level approach for characterizing water-insoluble components of ambient organic aerosol particulates using ultrahigh-resolution mass spectrometry. Atmos. Chem. Phys. 14, 10299–10314.

Win, M.S., Tian, Z., Zhao, H., Xiao, K., Peng, J., Shang, Y., Wu, M., Xiu, G., Lu, S., Yonemochi, S., Wang, Q., 2018. Atmospheric HULIS and its ability to mediate the reactive oxygen species (ROS): a review. J. Environ. Sci. (China) 71, 13–31.

Wu, G., Wan, X., Gao, S., Fu, P., Yin, Y., Li, G., Zhang, G., Kang, S., Ram, K., Cong, Z., 2018. Humic-like substances (HULIS) in aerosols of central Tibetan Plateau (Nam Co, 4730 m asl): abundance, Light absorption properties, and Sources. Environ. Sci. Technol. 52, 7203–7211.

Zhao, M., Qiao, T., Li, Y., Tang, X., Xiu, G., Yu, J.Z., 2016. Temporal variations and source apportionment of Hulis-C in $PM_{2.5}$ in urban Shanghai. Sci. Total Environ. 571, 18–26.

Zheng, G., He, K., Duan, F., Cheng, Y., Ma, Y., 2013. Measurement of humic-like substances in aerosols: a review. Environ. Pollut. 181, 301–314.